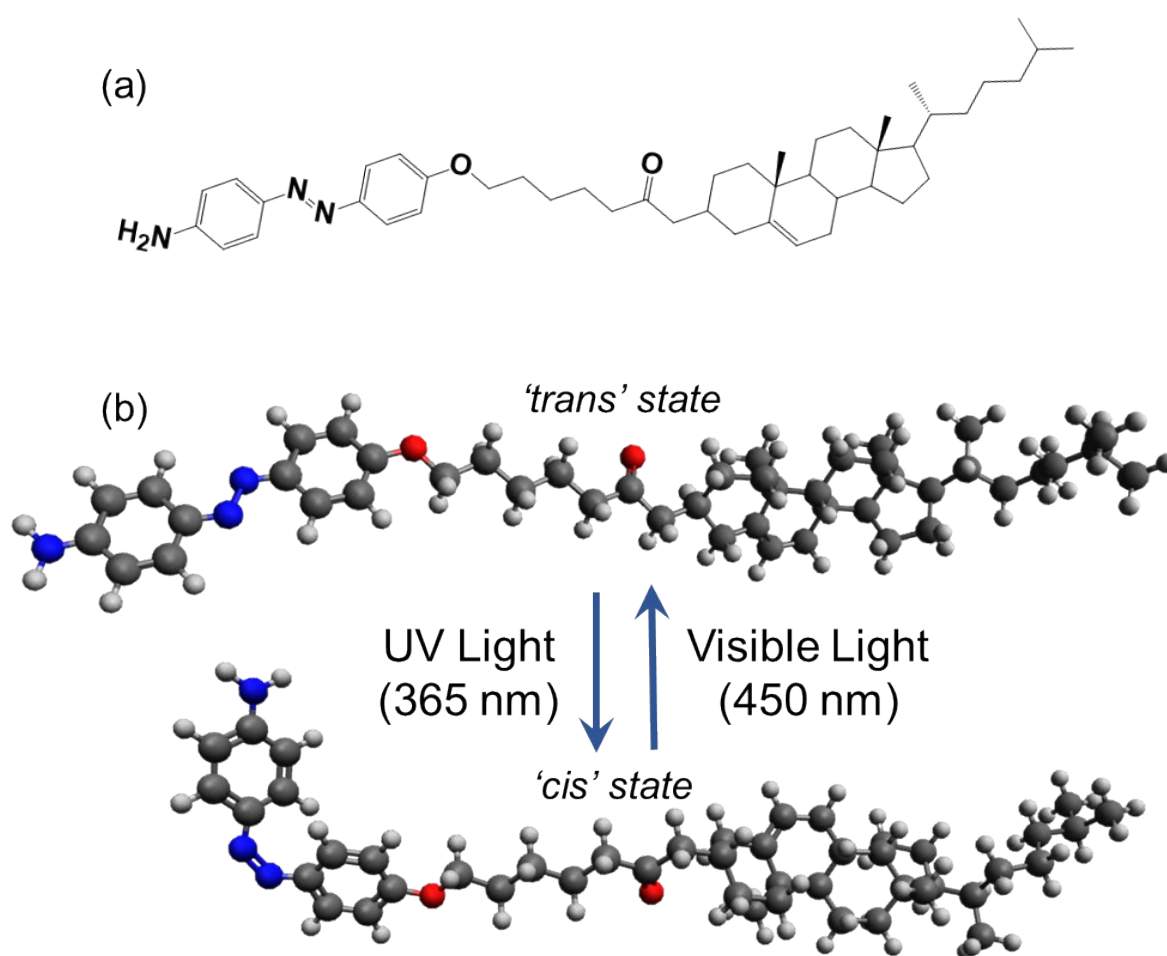


## Electronic Supplementary Information

### Photo-tunable Epsilon-Near-Zero behavior in a Self-assembled Liquid Crystal – Nanoparticle Hybrid Material

Amit Bhardwaj, Vimala Sridurai, Sachin A. Bhat, Channabasaveshwar V. Yelamaggad and Geetha G. Nair\*

#### S1. Chemical structure of the photo-active liquid crystal ligand (ALC):



**Figure S1:** (a) Chemical structure of the ALC in the pristine state and (b) ball -stick diagram of the 'trans' and 'cis' isomers of ALC in the pristine and UV-irradiated cases respectively.

#### S2. AFM studies:

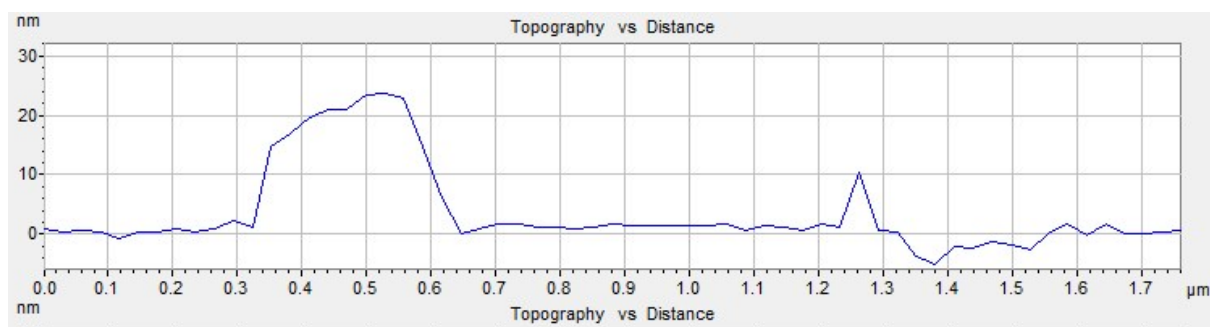
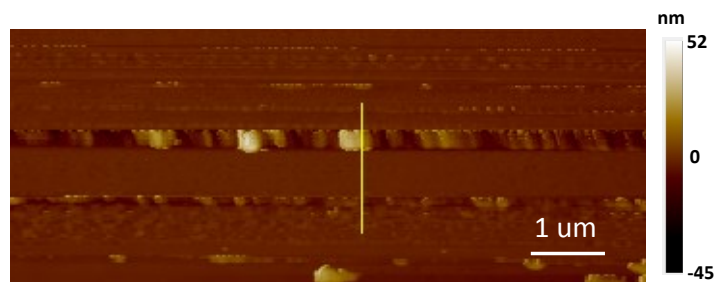


**Figure S2:** (Top) The surface topography image of the GNP-ALC sample deposited on Si substrate obtained from AFM. The thickness of the film is calculated to be  $\sim 20$  nm from the (Bottom) 1-D profile of the image (across the yellow line).

### S3. Chemical and thermal characterization of the GNP-ALC system:

#### (i) NMR studies:

$^1\text{H}$  and  $^{13}\text{C}$  NMR is recorded in the solution ( $\text{CDCl}_3$ ) for both the ligand (ALC) and the composite (GNP-ALC). The spectra obtained for the ligand ALC are shown in Figure S3. It is observed that the  $^1\text{H}$  spectra for ALC show four doublets one at significantly upfield compared to other, indicating the presence of strong electron donating  $-\text{NH}_2$  and alkoxy groups. The peaks corresponding to cholesterol are found to be in agreement with the theoretical values[R1], indicating the formation of pure ALC which was further used for the synthesis of GNP-ALC.

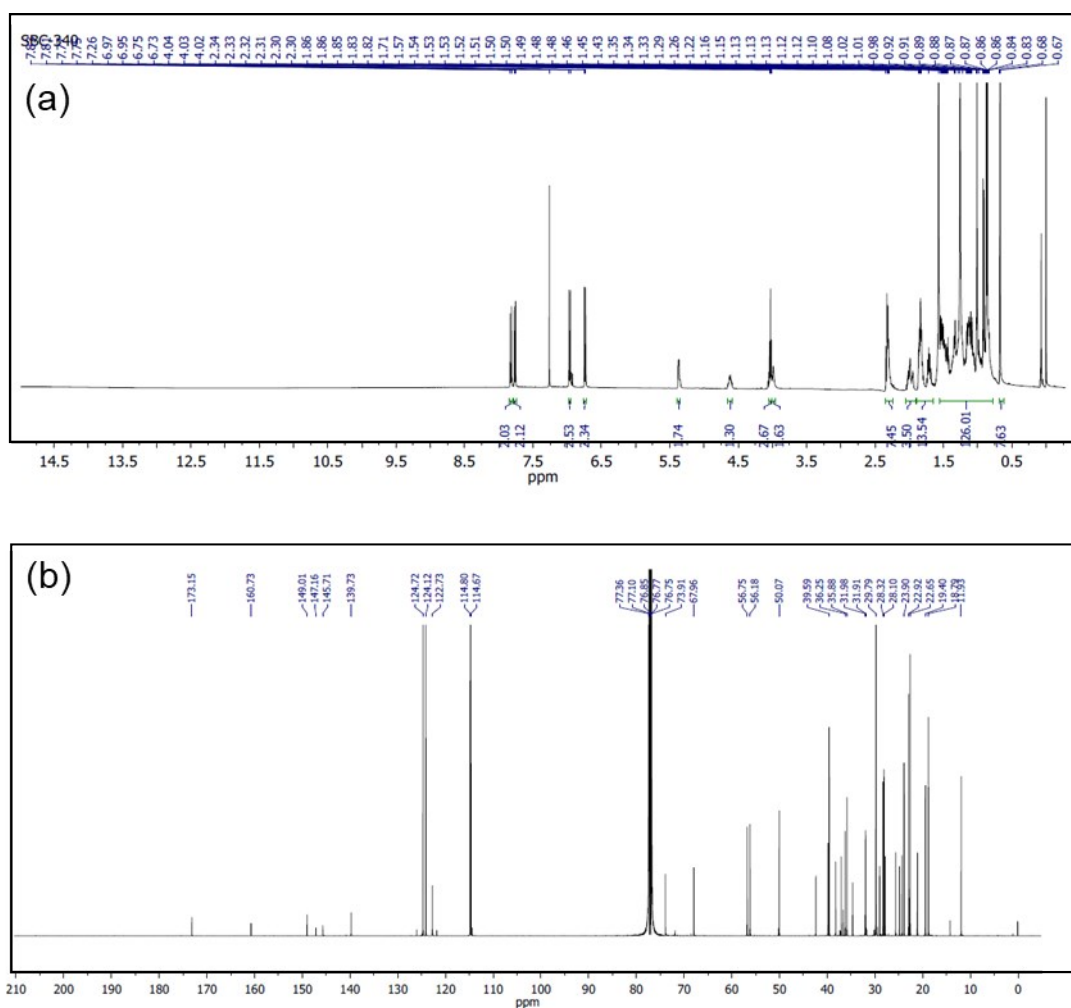


**Figure S3:** (a)  $^1\text{H}$  (400 MHz,  $\text{CDCl}_3$ ) and (b)  $^{13}\text{C}$  (100 MHz,  $\text{CDCl}_3$ ) NMR spectra for the ligand (ALC)

The NMR spectra of GNP-ALC are shown in Figure S4. The spectral pattern is quite similar to that of ALC but as can be seen from the image, the peaks are slightly diffused in nature[R1]. Its clear from the NMR that even after the formation of GNP-ALC, the spectral pattern and positions remain similar indicating the presence of ligands which are structurally intact even after attaching with the GNP nanoparticles.

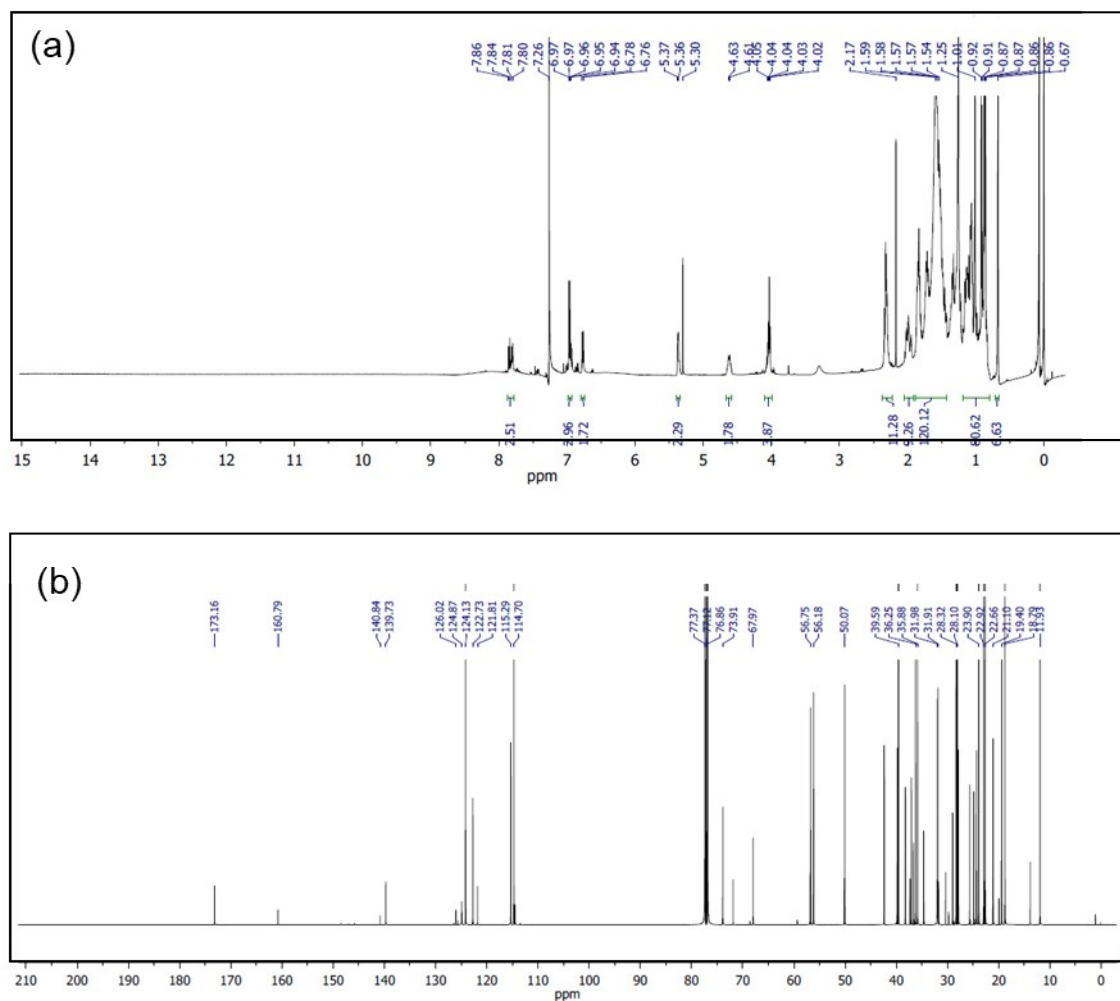


**Figure S4:** (a)  $^1\text{H}$  (400 MHz,  $\text{CDCl}_3$ ) and (b)  $^{13}\text{C}$  (100 MHz,  $\text{CDCl}_3$ ) NMR spectra for the compound (GNP-ALC)

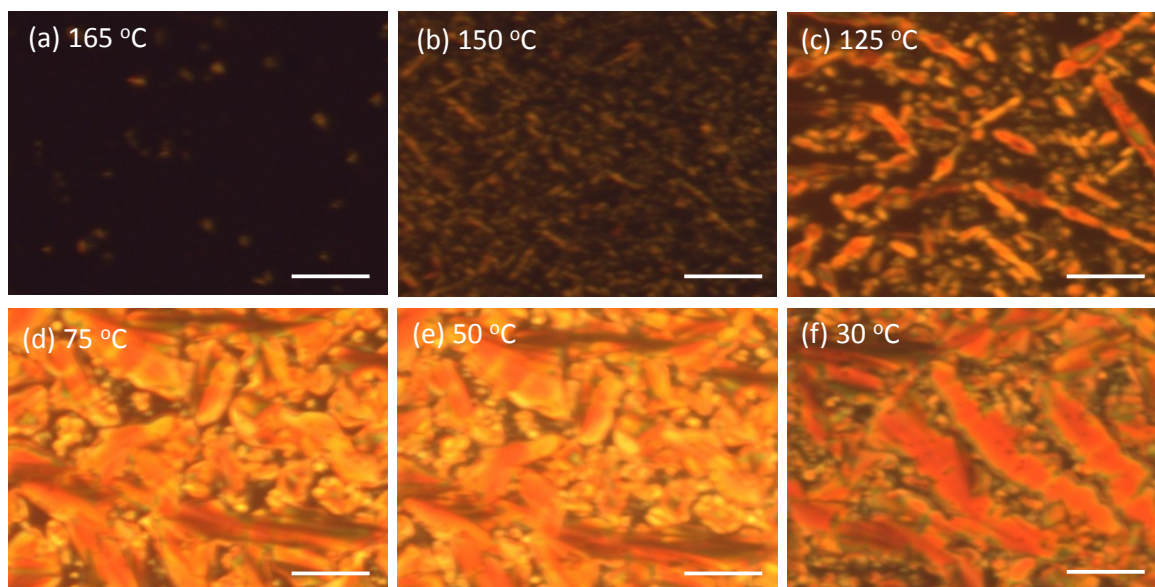


*Figure S5: POM texture of the GNP-ALC sample observed between polyimide coated glass substrates in the cooling cycle. Scale bar is 25  $\mu\text{m}$ .*

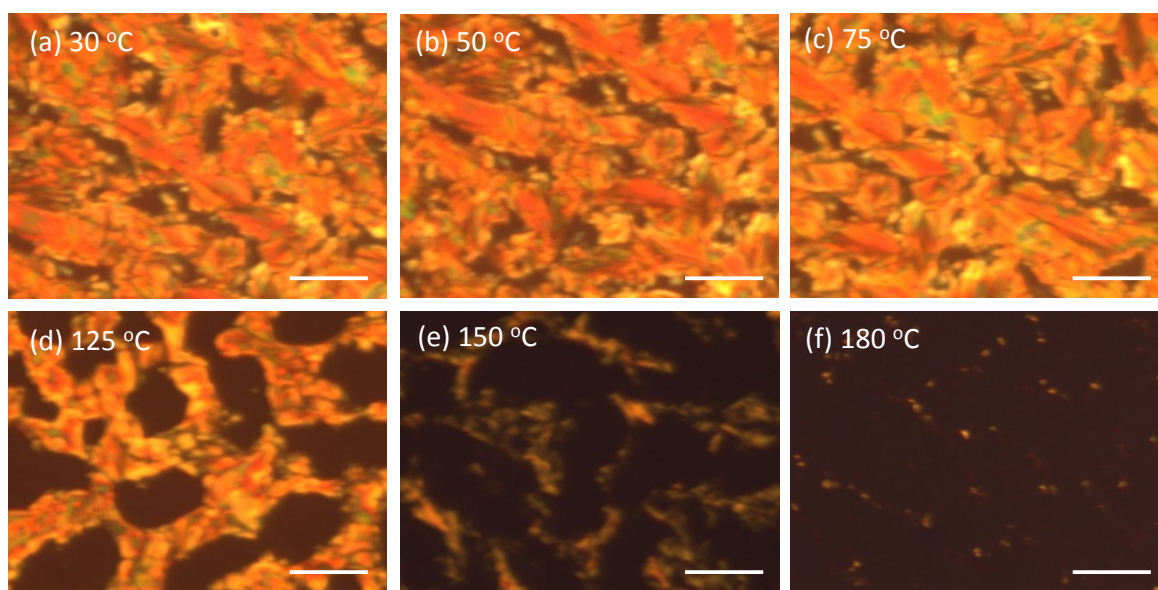


*Figure S6: POM texture of the GNP-ALC observed between polyimide coated glass substrates in the second heating cycle. Scale bar is 25  $\mu\text{m}$ .*

**(ii) POM observations:**

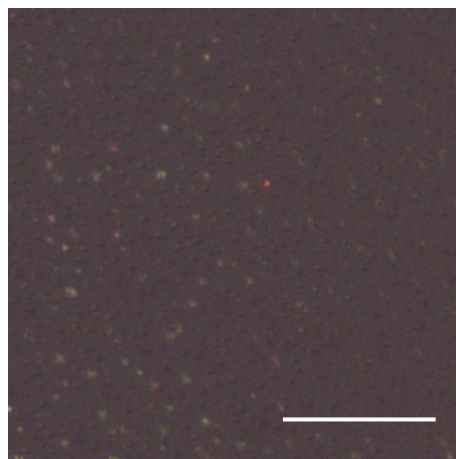


Figure S7: POM texture of the GNP-ALC sample spin coated on silicon substrate at room temperature, exhibiting predominantly homeotropic alignment. Scale bar is 20  $\mu\text{m}$ .

**(iii) TGA:**

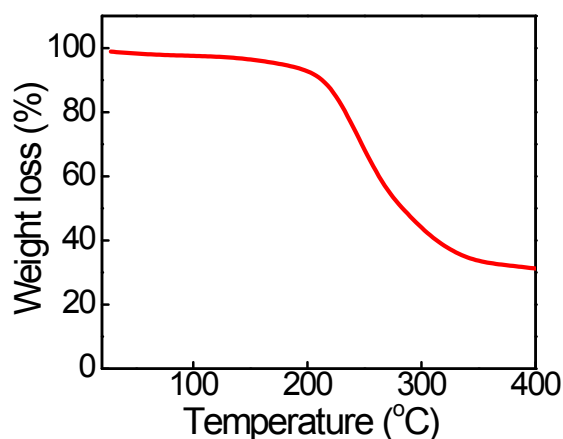
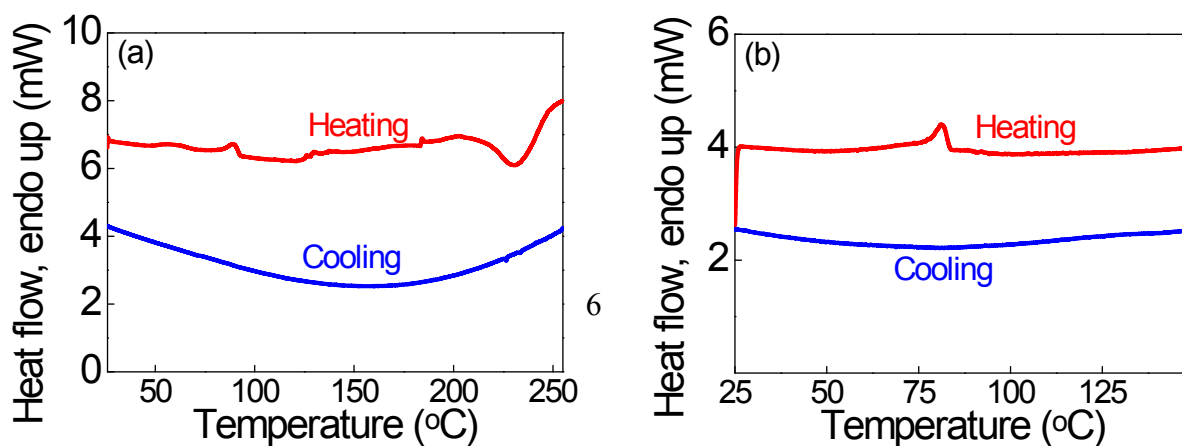


Figure S8: TGA trace of the compound GNP-ALC

**(iv) Differential scanning calorimetry (DSC):**

DSC thermograms obtained in the 1st heating and cooling cycles are shown in Figure S9a. The dip observed in the heating cycle in the thermal range 200-250 °C is a clear indication of sample degradation. This also confirms the results obtained from the TGA studies (see Figure S8 and discussion in Morphological and structural characterization section of the main manuscript)



which indicate that the sample degrades at  $\sim 225$  °C. Further DSC studies are carried out on a fresh as-synthesized sample in the heating and cooling cycles at 5 °C/min rate to confirm the thermal range of the mesophase. In this case, the sample is heated only up to 150 °C to avoid the sample degradation. The DSC profile (Figure S9b) shows the melting transition (crystal to mesophase) in the thermal range of 80 to 90 °C, corroborating the POM observation. The mesophase is stable through the thermal range starting from 150 °C to  $\sim 25$  °C on cooling, and no signature of any other phase transition or crystallization peak is seen in the thermogram up to ambient temperatures.

**Figure S9:** DSC profiles of the compound GNP-ALC in both heating (1st heating) and cooling cycles ramping 5 °C/min.

#### S4. Circular dichroism studies:

Circular dichroism (CD) experiments are carried out on both ALC and GNP-ALC to study their macroscopic chirality and compare the helical sense (left/ right handedness) between the two compounds. The thermal dependence of the CD spectra obtained in the cooling cycle is shown in Figure S10. The ALC which exhibits a chiral nematic (N\*) phase (from POM studies), shows CD activity throughout the thermal range of the mesophase, i.e. 180 °C to 120 °C. With a decrease in wavelength, the optical rotation is positive and then crosses zero to become negative (See Figure S10a). This is a signature of the positive ‘Cotton effect’ with a positive 1<sup>st</sup> and negative 2<sup>nd</sup> Cotton peaks. Such a feature indicates the left-handed helicity of the system [R2, R3]. Upon further cooling, the sample crystallizes, and CD activity disappears, as seen at 35 °C.

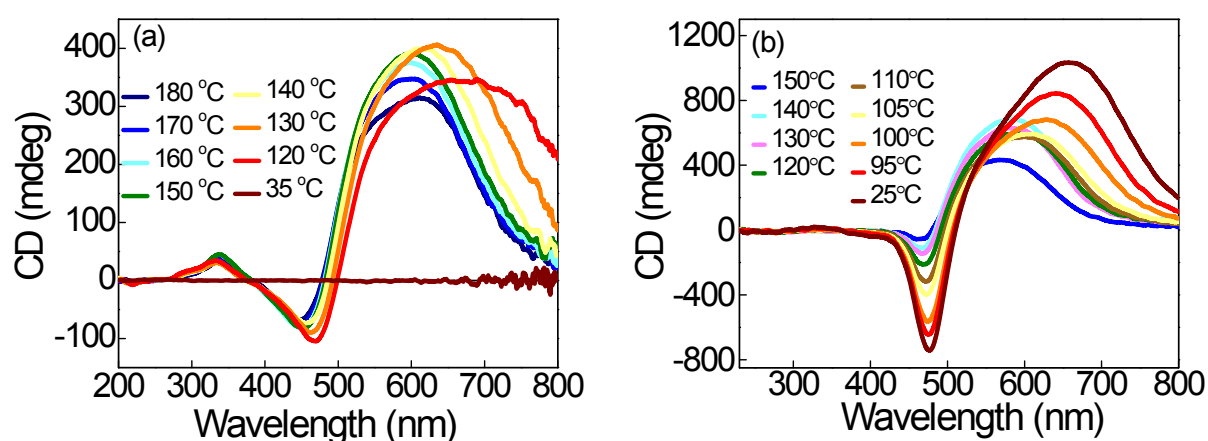


**Figure S10:** Thermal dependence of the circular dichroism profiles of (a) ALC and (b) GNP-ALC obtained in the thin film state in cooling cycle. The profiles for GNP-ALC indicate a left-handed helical structure with the helicity enhancing upon decreasing temperature.

In the case of GNP-ALC, CD activity is observed (see Figure S10b) through the entire thermal range of the lamellar mesophase, starting from 150 °C to 25 °C. Also the sample exhibits positive ‘Cotton effect’ and the left handed helicity similar to ALC, indicating that the macroscopic chirality and helical sense of the ligand are retained in the GNP-ALC. Further, the negative peak becomes more prominent upon cooling which indicates the enhancement of helicity deeper in the lamellar phase.

### S5. UV-visible spectroscopy (solution state):

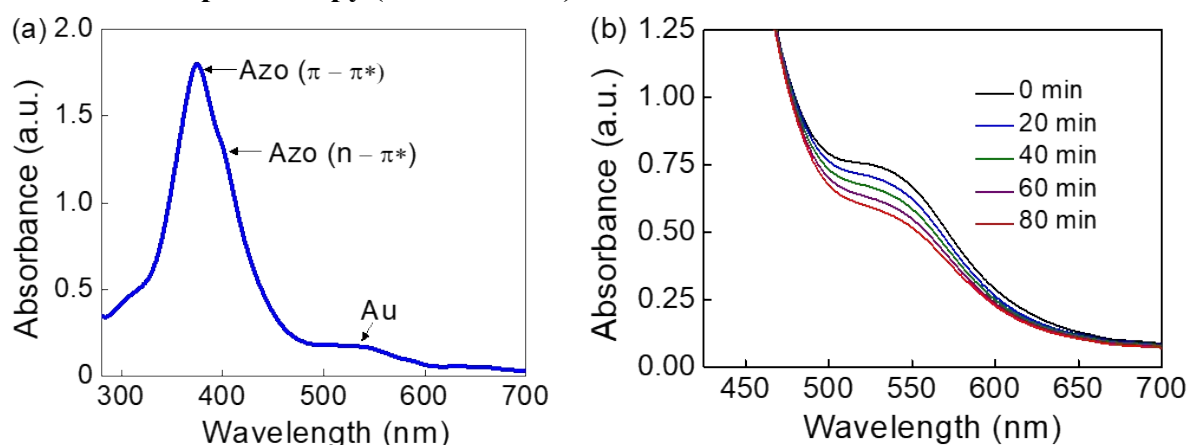


**Figure S11:** UV-Visible spectra in the (a) pristine and (b) UV irradiated states of GNP-ALC system dissolved in DCM. The spectrum corresponding to the pristine state in (a) also shows a peak at  $\sim 520$  nm corresponding to the LSPR peak of Au which (b) red-shifts on illumination with UV light.

### S6. Ellipsometry:

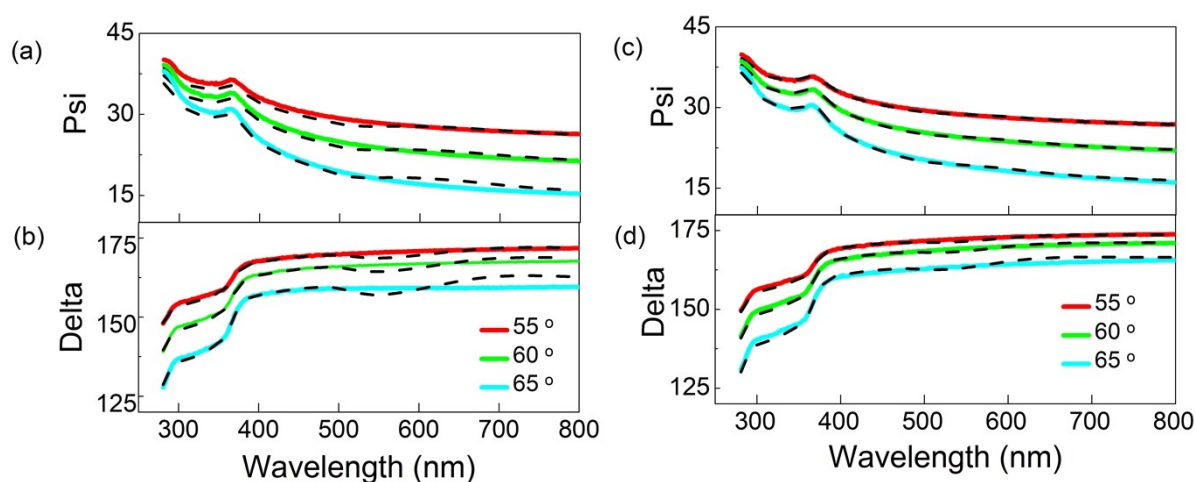




**Figure S12:** Psi and delta profiles obtained from ellipsometry for the (a & b) pristine and (c & d) UV-irradiated states respectively. The solid and dashed lines represent the experimental and fit data respectively.

### **S7. Effective medium parameters:**

The system is considered as a cubic lattice arrangement of Au nanoparticles of radius ( $r$ ) embedded in a liquid crystal medium (as discussed in the ‘epsilon-near-zero behavior’ section of the manuscript). The refractive index ( $n_m$ ) of the surrounding liquid crystal medium in the ‘trans’ state is considered to be 1.6 (the average refractive index of a typical liquid crystal in the optical regime). The permittivity ( $\epsilon_m$ ), and hence the refractive index of the LC ( $n_m$ ) are directly proportional to the dipole moment ‘M’ according to the relationship:

$$\epsilon_m = \frac{M^2}{K_B T}$$

Where,  $K_B$  and  $T$  correspond to the Boltzmann constant and temperature respectively. The dipole moments of the ligand in the ‘trans’ and ‘cis’ isomeric states of azobenzene calculated using the Avogadro (Ver 1.2.0) software are 4.613 D and 5.353 D, respectively.

#### ***Estimation of refractive index of the UV-irradiated state of the ALC medium:***

Considering the dipole moment values of the ‘trans’ and ‘cis’ isomers, the refractive index of the ALC in the ‘cis’ isomeric state is estimated as follows:

Dipole moment ( $M$ ) in ‘trans’ state = 4.613 D

$$\begin{aligned} \text{Permittivity } (\epsilon_m) \text{ in ‘trans’ state (considering absorption coefficient as zero)} &= (1.6)^2 \\ &= 2.56 \end{aligned}$$

Dipole moment ( $M$ ) in ‘cis’ state = 5.353 D

$$\begin{aligned} \text{Permittivity } (\epsilon_m) \text{ in ‘cis’ state} &= \frac{2.56}{4.613} \times 5.353 \\ &= 2.97 \end{aligned}$$

Corresponding refractive index ( $n_m$ ) in ‘cis’ state = 1.7

Thus, the refractive index of the surrounding LC medium in the ‘cis’ state is estimated to be 1.7.

#### ***Estimation of interparticle distance in the UV-irradiated state of the GNP-ALC system:***

Interparticle distance in the pristine ‘trans’ state (from XRD data) = 4.1 nm

Ligand length in ‘trans’ state (from Avogadro software) = 3.6 nm

Ligand length in ‘cis’ state (from Avogadro software) = 3.2 nm

GNP particle diameter (from TEM data) = 3.2 nm

Calculated interlayer distance in the 'trans' state (GNP dia+ligand length in 'trans' state)

$$= 3.2 + (2 * 3.6)$$

$$= 10.4 \text{ nm}$$

Calculated interlayer distance in the 'cis' state (GNP diameter + ligand length in 'cis' state)

$$= 3.2 + (2 * 3.2)$$

$$= 9.6 \text{ nm}$$

The difference in interlayer distance (calculated) between 'trans' and 'cis' states =  $10.4 - 9.6$

$$= 0.8 \text{ nm}$$

Hence, the estimated interparticle distance in 'cis' state  $\sim 4.1 - 0.8$

$$\sim 4 \text{ nm}$$

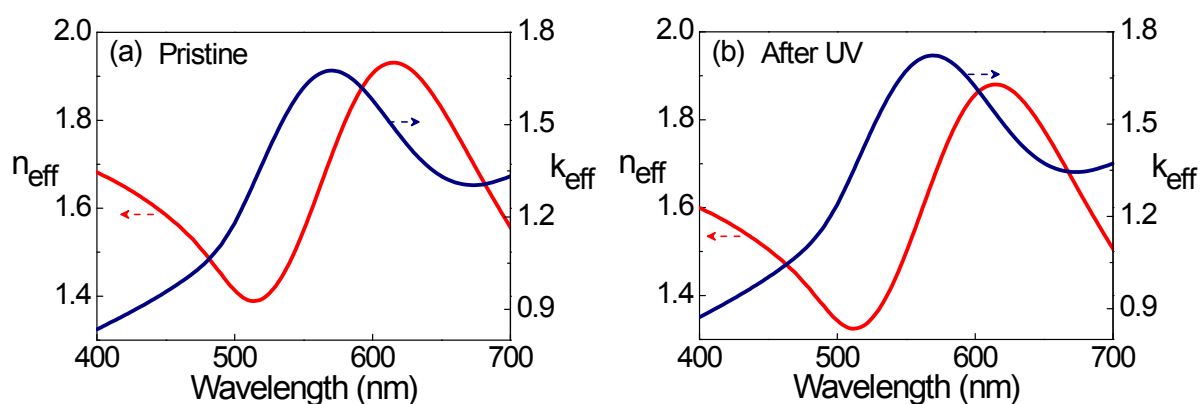


**Figure S13:** The optical constants ( $n_{\text{eff}}$  &  $k_{\text{eff}}$ ) extracted from the ellipsometry data ( $\psi$  and  $\Delta$ ) in the (a) pristine and (b) UV irradiated states.

### Supporting Information References

[R1] L. Cseh, X. Mang, X. Zeng, F. Liu, G. H. Mehl, G. Ungar, G. Siligardi, *J. Am. Chem. Soc.* **2015**, *137*(40), 12736–12739.

[R2] G. Gottarelli, S. Lena, S. Masiero, S. Pieraccini, G. P. Spada, *Chirality* **2008**, *20*, 471–485.

[R3] G. Gottarelli, G. P. Spada, E. Castiglioni, in *Molecular Gels*, ed. Weiss R.G.; Terech, P. Springer: Dordrecht, **2006**, Ch. 13, pp. 837-850.

